ISSN 2304-3415, Russian Open Medical Journal
2020. Volume 9. Issue 1 (March). Article CID e0105
DOI: 10.15275/rusomj.2020.0105

Original article

Relationships between myocardial perfusion abnormalities and integrated indices of atherosclerotic burden: clinical impact of combined anatomic-functional evaluation

Konstantin V. Zavadovsky [1], Alina N. Maltseva [1], Elena V. Grakova [1], Kristina V. Kopeva [1], Marina O. Gulya [1], Victor V. Saushkin [1], Andrew V. Mochula [1], Riccardo Liga [2], Alessia Gimelli [3]

[1] Cardiology Research Institute, Tomsk National Research Medical Centre, Russian Academy of Science, Tomsk, Russia
[2] University Hospital of Pisa, Pisa, Italy
[3] Fondazione Toscana G. Monasterio, Pisa, Italy

Received 21 October 2019, Accepted 26 January 2020

Abstract: *Aim* to evaluate the relationships between functional and anatomical information obtained by myocardial perfusion imaging (MPI) and coronary computed tomography angiography (CCTA) in a series of consecutive patients at intermediate probability of coronary artery disease (CAD).
Material and Methods — The study group comprised 139 patients (83 men, age of 61.6±7.5 years) who underwent CCTA and single-photon emission computed tomography myocardial perfusion imaging (SPECT-MPI). Based on CCTA results patients were divided into three groups: 1) with the absence of coronary atherosclerosis on CCTA; 2) with non-obstructive CAD (<50%); 3) with obstructive (≥50%) CAD. The Segment Involvement Score, Segment Stenosis Score (SSS) and CTA Risk Score were calculated as measures of global atherosclerosis burden. MPI studies were considered abnormal in the presence of SSS≥4.
Results — Abnormal myocardial perfusion was detected in 60% of cases in group 1 and 2; in 75% of cases in group 3. The overall frequencies of normal and abnormal MPI studies differed significantly only in obstructive CAD patients and did not differ in group 1 and 2. There were no significant correlations between calcium score, atherosclerotic lesion length, positive remodelling index and MPI results in patients with non-obstructive as well as in patients with obstructive CAD. In group of patients with obstructive CAD Segment Stenosis Score correlated wekly with SSS (r=0.39, p=0.001) and SDS (r=0.28; p=0.012); the CTA Risk Score showed correlationes with SSS (r=0.38, p=0.002) and SDS (r=0.30, p=0.020).
Conclusion — Myocardial perfusion abnormalities may develop even in the absence of critical coronary artery lesions. The extent of myocardial ischemia correlates with measures of global CAD burden only in patients with obstructive CAD.

Keywords: coronary artery disease, myocardial ischemia, atherosclerosis, computed tomography, myocardial perfusion imaging.

Cite as Zavadovsky KV, Maltseva AN, Grakova EV, Kopeva KV, Gulya MO, Saushkin VV, Mochula AV, Liga R, Gimelli A. Relationships between myocardial perfusion abnormalities and integrated indices of atherosclerotic burden: clinical impact of combined anatomic-functional evaluation. *Russian Open Medical Journal* 2020; 9: e0105.

Correspondence to Konstantin Konstantin V. Zavadovsky. Address: Cardiology Research Institute, Tomsk National Research Medical Centre, Russian Academy of Science, Kievskaya str. 111A, Tomsk, 634012, Russia. Phone: +73822558298, +79039518791. Fax: +73822555057. E-mail: konstzav@gmail.com.

Introduction

Nuclear cardiology and coronary computed tomography angiography (CCTA) imaging are included in the management flow charts of patients with chest pain and suspected coronary artery disease (CAD), providing complementary insight into coronary anatomy and function. Specifically, myocardial perfusion imaging (MPI) with single photon emission computed tomography (SPECT) is still the most performed non-invasive imaging modality for the evaluation of myocardial perfusion, allowing to assess the functional severity of a given coronary stenosis and to perform an in-depth characterization and risk stratification of patients with ischemic heart disease (IHD) [1]. On the other hand, CCTA has become the reference standard for the non-invasive assessment of coronary anatomy, allowing to readily quantify coronary stenosis severity, assess the plaque structure and to exclude accurately the presence of anatomically obstructive CAD. However, despite its widespread diffusion in the clinical arena, CCTA is unable (except when using fluid dynamic analysis) to assess the functional significance of coronary lesions, possibly leading to the over-diagnosis of CAD, and posing the conditions for the inappropriate referral of patients to invasive procedures and revascularizations [2].

The combination of coronary anatomic and functional information as provided by integrated CCTA/MPI imaging could allow the evaluation of the regional interaction between CAD and downstream myocardial perfusion abnormalities, guiding patients clinical management. In this context, while focal coronary stenosis and diffuse CAD may both impair profoundly regional myocardial perfusion [3], a detailed evaluation of their relative effect on myocardial perfusion abnormalities in patients submitted to combined CCTA/MPI assessment has not been fully explored.

The aim of this study was to evaluate the relationships between functional and anatomical information obtained by MPI and CCTA in a series of consecutive patients at the intermediate probability of CAD. Moreover, a detailed analysis of atherosclerotic burden indices versus MPI results was obtained, in order to explore the relative impact of diffuse atherosclerosis on the myocardial ischemic burden.

Material and Methods

Study population and study design

Between June 2015 to August 2016 in our department, 660 CCTA and 1770 SPECT-MPI were performed. From them we retrospectively selected patients with the following criteria: 1) age >21 years; 2) intermediate (15-85%) pre-test probability of stable CAD [4]; 3) who underwent both CCTA and MPI SPECT within not more than 7 days without any invasive interventions and/or clinical events in this period. The reasons for the second noninvasive test were: unclear results of the first test or the myocardial perfusion assessment in cases of moderate and severe coronary artery stenosis.

Exclusion criteria were as follows: contraindication to adenosine or iodine administration, hemodynamic instability, acute coronary syndrome, myocardial inflammatory diseases, storage diseases, moderate-to-severe cardiac valvular disease, renal insufficiency (serum creatinine level >1.5 mg/dl), atrial fibrillation, ventricular arrhythmias (grade III-V according to the Lown's classification), known CAD (previous myocardial infarction (MI) or revascularization).

Based on forementioned criteria a total of 139 patients were selected.

To assess myocardial perfusion patterns depending on the results of the CCTA all patients were divided into three groups: 1) with the absence of coronary atherosclerosis on CCTA; 2) with angiographically non-obstructive CAD (at least one <50% stenosis in one or more coronary arteries and the absence of CA stenosis ≥50%); 3) with obstructive (≥50%) CAD.

Patient preparation and protocols

All CT and SPECT studies were performed using hybrid system (GE Discovery NM/CT 570C; GE Healthcare, Milwaukee, WI, USA) equipped with dedicated cardiac Cadmium-Zinc-Telluride (CZT) gamma camera and 64-slice CT scanner.

CT coronary angiography. An unenhanced coronary artery calcium scoring scan was obtained according to the following protocol: prospective triggering at 75% of R-R interval; tube voltage of 120 kV; tube current of 435 mA.

Heart rate and blood pressure were evaluated before each scan. Patients with a heart rate higher than 60 bpm were treated with intravenous infusion of 1mg metoprolol before CT scan and all patients received 0.5 mg of sublingual nitroglycerin.

For the contrast-enhanced scans, 70-90 mL of non-ionic contrast agent (Iopamidol 370 mg iodine/mL, Bracco Diagnostics, Italy) was injected intravenously through an 18-gauge antecubital catheter at a flow rate of 5-5.5 mL/s followed by 40 mL of saline.

In patients with heart rate ≥55 bpm a helical scan with retrospective ECG gating protocol was used and in those with heart rate <55 the prospective ECG gating protocol was performed. The acquisition parameters were as follows: tube voltage of 120 kV; tube current of 300-600 mA using ECG modulation with maximum tube current between 40-80% phases and minimum tube current in remaining phases. Estimated radiation doses ranged from 1,5-3 mSv by using retrospective synchronisation and 10 to 25 mSv in cases of prospective synchronisation.

Myocardial perfusion imaging

Stress protocols. Patients were instructed to refrain from caffeine and methylxanthine-containing substances and to avoid nitrates, calcium channel blockers and beta-blockers for at least 24 h before the scan. All scans were performed after an overnight fasting.

Pharmacologic stress testing with adenosine was performed in all patients. Adenosine was administered intravenously at 140 mcg/kg/min for 6 min, and the radiopharmaceutical was injected at the end of minute 3 [5]. The heart rate, systemic blood pressure, and 12-lead electrocardiogram (ECG) were monitored before, throughout, and after the infusion of vasodilator. Pharmacologic stress testing did not lead to atria-ventricular conduction delay and/or to ST segment depression in any patient.

All patients underwent a two-day stress-rest ECG-gated MPI on a solid-state detector CZT cardiac gamma camera (GE Discovery NM/CT 570C). Myocardial perfusion imaging (MPI) scans were acquired using low-energy multi-pinhole collimator and 19 stationary detectors simultaneously imaging 19 different views without detector rotation. Each detector contained 32×32 pixelated (2.46×2.46 mm) CZT elements. 20% energy window at 140 keV was used. The images were acquired 60 min after ^{99m}Tc-sestamibi (370 MBq) injection for both the stress and rest studies. All patients were imaged in the supine position with arms placed over their heads. The acquisition time was 7 min. The mean ^{99m}Tc-MIBI dose at rest was 370 MBq at stress and stress.

CT attenuation correction. To obtain attenuation map, low-dose unenhanced CT scan without ECG triggering and breath-hold was performed in all patients with the following parameters: tube voltage of 120 kV, tube current of 20 mA, rotation time of 0.8 s, helical pitch 0,969:1, slice thickness of 5 mm, and interstice interval of 5 mm for both stress and rest [6].

Data analysis

All CCTA images were interpreted by two experienced readers blinded to MPI results. Discrepancies in interpretations were resolved by consensus. Axial images, curved multiplanar reformations, and thin-slab maximum-intensity projections were used for dataset analysis on the dedicated workstation (Advantage Workstation 4.6; GE Healthcare).

Coronary artery calcium analysis. Coronary artery calcium score was calculated with dedicated SmatScore 4.0 software (Advantage Workstation; GE Healthcare) according to the method of Agatston *et al.* [7].

Coronary CTA image analysis. In the case of retrospective CCTA scans, images were reconstructed at 75% of the cardiac cycle with slice thickness of 0.625 mm. In cases of heart rate artefacts, other reconstruction windows were used (from 40% to 65% of the *R-R* cycle). All coronary artery segments were analyzed and divided into four levels of quality as follows: level 1: excellent quality (absence of motion, heart rate, and other artefacts; clear delineation of vascular contours); level 2: good quality (non significant artefacts, minimal blurring of vascular structures); level 3: adequate quality (moderate artifacts and/or blurring); and level 4: poor quality (significant artefacts and/or blurring; not

evaluative). Only segments without significant artefacts (levels 1 to 3) were used for further analysis (1421/1480, 96%). According to Heart Association Modified Classification, coronary arteries were subdivided into 16 segments [8]. Only segments with a diameter of ≥2.0 mm were included. In each segment, a degree of stenosis was measured in cross-section and curved multiplanar reconstructions.

Beyond the stenosis severity the following plaque characteristics were assessed: Agatston calcium score, positive remodelling index [9], total atherosclerotic lesion length, plaque structure (soft-tissue, mixed or calcified).

For the global atherosclerosis burden assessment, three previously established integrated indexes were assessed: computed tomographic angiography (CTA) Risk Score, Segment Involvement Score and Segment Stenosis Score. CTA Risk Score was calculated based on the stenosis location, severity and plaque structure [10]. The Segment Involvement Score was calculated as the total number of coronary artery segments with atherosclerotic plaques regardless of the degree of stenosis [11]. Also the Segment Stenosis Score was calculated. For this, each coronary segment was graded using a 5-point scoring system (0 = no plaque; 1=1-24% stenosis; 2=25-49% stenosis; 3 = 50-69% stenosis; and 4=≥70% stenosis) [12].

SPECT data processing. All MPI images were interpreted by two experienced nuclear cardiology physicians. Low dose CT scans were transferred on a Xeleris workstation to obtain attenuation maps for attenuation correction.

The attenuation correction process was described in [13]. The quality control was performed visually by an alignment of CT and SPECT images of the LV. CZT images were reconstructed on the dedicated workstation (Xeleris 4.0; GE Healthcare, Haifa, Israel) using maximum-penalized-likelihood iterative reconstruction (60 iterations; Green OSL Alpha 0.7; Green OSL Beta 0.3) to acquire perfusion images in standard cardiac axes (short axis, vertical long axis, and horizontal long axis). The software Myovation for Alcyone (GE Healthcare, Haifa, Israel) was used for image reconstruction, and Butterworth post-processing filter (frequency 0.37; order 7) was applied to the reconstructed slices. The reconstruction was performed in 70×70 pixels matrix with 50 slices.

MPI data analysis. Raw MPI-CZT data at stress and at rest were visually analysed for motion and attenuation artefacts. Stress/rest images were analysed with a commercially available software package Corridor 4DM (University of Michigan, Ann Arbor, MI, USA). The calculation of MPI parameters was performed based on uncorrected and attenuation corrected image analysis.

Perfusion in each of 17 segments was visually classified as 0=normal, 1=mild reduction, 2=moderate reduction, 3=severe reduction or 4=absent perfusion, and the segmental scores were summed for the stress (SSS) and rest (SRS) images. The difference between SSS and SRS was calculated as the summed difference score (SDS). MPI studies were considered abnormal in the presence of SSS≥4 [14]. Each perfusion defect was assigned to one or more coronary territories according to the standardized myocardial segmentation model.

The results of CCTA were used for coronary dominance assessment. In patients with the left coronary dominance, the inferior (4, 10, 15) and infero-lateral (5, 11) segments were assigned to the LCx territory, and all four apical segments (13, 14, 16 and 17) were assigned to the left anterior descending territory. In patients with the right dominant coronary system, the inferior (4, 10), inferolateral (5, 11), and apical inferior (15) segments were assigned to the RCA territory. Remaining four apical segments (13, 14, 16, and 17) were assigned to the LAD artery territory [15].

Statistical analysis

The distribution of continuous variables was checked by using the Shapiro-Wilk W-test. Continuous variables were expressed as mean with standard deviation (M±SD) and as median with interquartile range (IQR). Categorical variables were presented as numbers and percentages – n (%). Group comparisons were performed using the nonparametric Kruskal–Wallis test. Statistical comparisons between two groups were performed by the Mann—Whitney U-test. Categorical variables were compared using the Fisher's exact test. Spearman test was used to estimate the correlation coefficient between quantitative variables. All tests were 2-sided; a $p<0.05$ was considered to be significant. Statistical analyses were performed using SPSS statistical software 19.0 (SPSS Inc., Chicago, IL, USA) and Medcalc version 17.4 (MedCalc Software, Mariakerke, Belgium).

Results

Patient characteristics

According to including and excluding criteria the were selected 139 patients, whose characteristics are presented in *Table* 1.

Pre-test CAD probability was 15-65% in 95 (68%) and 66-85% in remaining 44 (32%) patients. Most of the patients had hypertension (80%), half of them had hypercholesterolemia and just under a third diabetes mellitus. Interestingly, among the 12 patients with normal results of CCTA and abnormal MPI all had pretest probability of CAD more >65% and hypertension (two of them with hypertensive crisis), 9 (75%) had diabetes mellitus**.**

Table 1. Characteristics of the study population (n=139)

Parameters	*Value*
Gender, M/F, n	83/56
Age, years, M±SD	61.6±7.5
Risk factors for CAD	
Diabetes mellitus (type 2), n (%)	39 (28%)
Hypertension, n (%)	112 (80%)
Hypercholesterolemia, n (%)	65 (47%)
Positive family history, n (%)	32 (23%)
Current smoking, n (%)	23 (17%)
Obesity (BMI ≥30 kg/m^2), n (%)	89 (64%)
Symptoms	
Dyspnea, n (%)	12 (9%)
Nonanginal chest pain, n (%)	58 (42%)
Atypical angina pectoris, n (%)	35 (25%)
Typical angina pectoris, n (%)	46 (33%)
Pretest likelihood of CAD	
Intermediate (15-65%), n (%)	95 (68%)
Intermediate (66-85%), n (%)	44 (32%)
Coronary calcium score (Agatston)	
0, n (%)	37 (27%)
1–99, n (%)	42 (30%)
100–399, n (%)	33 (24%)
≥400, n (%)	27 (19%)

M±SD, mean with standard deviation; numbers and percentages – n (%); M, male; F, female; CAD, coronary artery disease; BMI, body mass index.

Table 2. Characteristics of myocardial perfusion disturbances depending on coronary artery stenosis degree

	All patients (n=139)	*Group 1 (n=20)*	*Group 2 (n=54)*	*Group 3 (n=65)*	*Kruskal-Wallis test p-value*	*Mann Whitney test p-value*		
						Group 1 vs Group 2	Group 1 vs Group 3	Group 2 vs Group 3
SSS	5.0 (3.0; 9.0)	4.5 (2.5; 7.0)	4.0 (3.0; 6.0)	8.0 (4.0; 11.0)	p=0.0016	p=0.804	p=0.009	p=0.001
SRS	1.0 (0; 3.0)	1.0 (0; 2.0)	1.0 (0; 3.0)	2.0 (1.0; 3.0)	p=0.0079	p=0.898	p=0.020	p=0.010
SDS	4.0 (3.0; 7.0)	4.0 (6.0; 6.5)	3.0 (2.0; 5.0)	6.5 (3.0; 9.0)	p=0.0008	p=0.229	p=0.087	p=0.001

SSS, summed stress score; SRS, summed rest score; SDS, summed difference score.

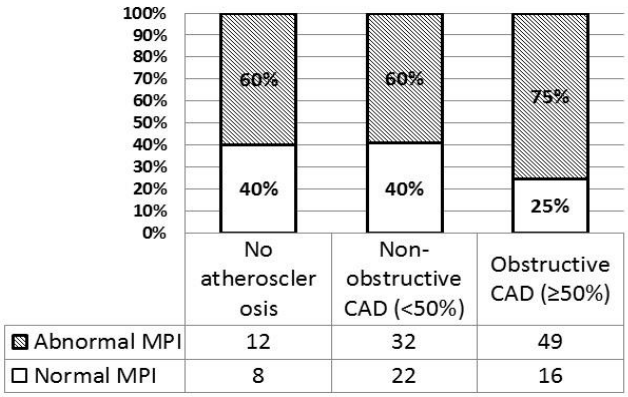

Figure 1. The percentage of normal and abnormal MPI in patients wihtout coronary atherosclerosis, with non-onstrictive and obstructive CAD.

Evaluation of anatomical results

Segment-based analysis showed that there were 471 segments with atherosclerotic plaques: 32 (7%) in the LM, 225 (48%) in the LAD, 103 (22%) in the LCx, and 111 (23%) in the RCA.

Over all coronary arteries, the average Segment Involvement Score was 4.0 (IQR 2.0, 6.0); Segment Stenosis Score was 7.5 (IQR 3.0, 13.0); CTA Risk Score 11.4 (IQR 5.9, 17.2).

There were 135 (25%) soft-tissue, 88 (16%) mixed and 320 (59%) calcifed atherosclerotic plaques. The total coronary calcium score was 83 (interquartile range 0.0; 320.0) Agatston units. 37 (27%) patients had calcium score 0; 42 (30%) patients - coronary calcium score 1-99; 33 (24%) patients coronary calcium score 100-399 and 27 (19%) of patients had coronary calcium score ≥400 Agatston units.

Obviously, the values all integrated indexes of coronary atherosclerosis in the group 1 were equal to zero. In the patients with obstructive CAD, compared with patients with non-obstructive CAD, the values of Segment Involvement Score {5.0 (IQR 4.0, 7.0) vs 3.0 (IQR 2.0, 5.0), p<0.001}, Segment Stenosis Score {12.0 (IQR 8.0, 16.0) vs 4.0 (IQR 3.0, 6.0), p<0.001} and CTA Risk Score {15.91 (IQR 12.0, 21.8) vs 9.8 (IQR 6.0, 13.6), p<0.001} were significantly higher. Moreover in patients wih ≥50% stenosis in comparison with <50% the following CCTA indexes were also significantly higher: calcium score {231.0 (83.0, 632.0) vs 41.5 (1.0, 176.0), p<0.001}, atherosclerotic lesion length {44.7 (26.2, 67.3) vs 15.4 (8.7, 33.7) mm, p<0.001} and positive remodelling index {6.13 (3.0, 8.2) vs 3.2 (1.4, 5.9), p=0.010}.

Functional versus anatomical results

Normal stress – rest MPI were observed in 46 (33%) patients (31 with pre-test probability 15-65% and 15 with pre-test 66-85% probability). Abnormal perfusion was found in the remaining 93 (67%) patients (65 and 28 with 15-65% and 66-85% pre-test probability, respectively).

The frequencies of normal and abnormal MPI in patients with the absence of coronary atherosclerosis, as well with non-obstructive and obstructive lesions are presented in *Figure* 1.

The frequencies of normal and abnormal MPI did not differ significantly in patients with the absence of coronary atherosclerosis as well with non-obstructive CAD. In the group of patients with ≥50% coronary artery stenosis, abnormal MPI (49 patients; 75%) was observed significantly more often than normal MPI (p=0.020).

It has been surprisingly found out that abnormal MPI results were observed more often even in patients with the absence of coronary atherosclerosis and in patients with non-obstructive lesions.

There was no significant correlation between such CCTA indexes as calcium score, atherosclerotic lesion length, positive remodelling index and MPI results as in patients with non-obstructive as in patients with obstructive CAD.

Detailed characteristic of myocardial perfusion abnormalities in different groups of patients is presented in *Table* 2. It was notable that moderate myocardial perfusion abnormalities were observed only in patients with CA stenosis ≥50%.

Relationships between myocardial perfusion abnormalities and integrated indices of atherosclerotic burden

Patient-based analysis. The Segment Involvement Score had only a weak correlation with SSS (r=0.19, p=0.004). The Segment Stenosis Score also showed weak correlations with SSS (r=0.29, p=0.001), SRS (r=0.25; p=0.005), and SDS (r=0.25, p=0.009). The CTA Risk Score showed weak correlations with SSS (r=0.21, p=0.004), SRS (r=0.20, p=0.029) and SDS (r=0.21; p=0.001).

Sub-group analysis. In patients with CA stenosis <50% neither Segment Involvement Score, Segment Stenosis Score nor the CTA Risk Score significantly correlated with MPI parameters.

In patients with ≥50% coronary artery stenosis, no correlation was found between the Segment Involvement Score and MPI parameters. In this group of patients Segment Stenosis Score correlated weakly with SSS (r=0.39, p=0.001) and SDS (r=0.28, p=0.012). The CTA Risk Score showed correlations with SSS (r=0.28, p=0.002) and SDS (r=0.30, p=0.020).

Vessel-based analysis. The regional Segment Involvement Score correlated with the LAD SSS (r=0.18, p=0.031). In the LAD territory, the regional Segment Stenosis Score had a weak correlation with SSS (r=0.23, p=0.005) and SDS (r=0.24, p=0.005). The CTA Risk Score in the LAD territory correlated with SSS (r=0.18, p=0.034) and SDS (r=0.21, p=0.022).

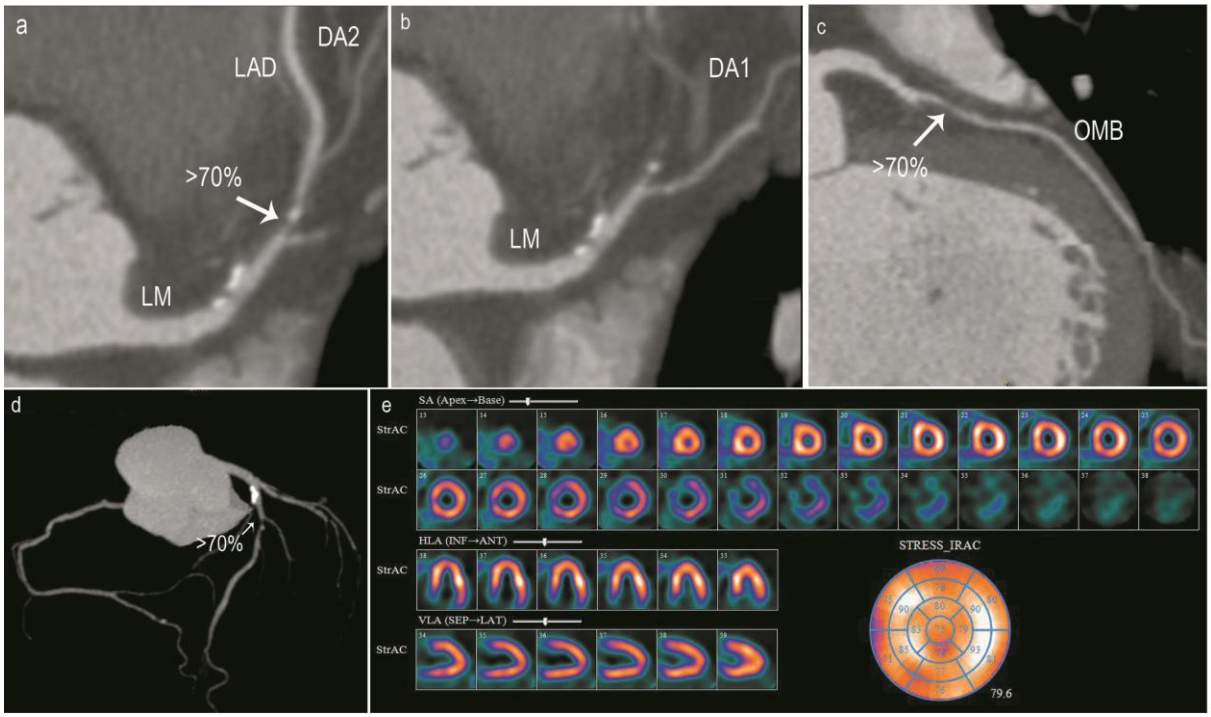

Figure 2. The example of discordance between CCTA and MPI results in 75-year-old man with atypical chest pain. Curved multiplanar reformations (a-c) and angiographic view (d) showing stenotic lesion in proximal segment of the LAD (a, e arrows) as well as in the OMB (c, arrow). Segment involvement score – 5; segment stenosis score – 13; CTA Risk Score 15.9. Post-stress SPECT images and polar map showing homogeneous myocardial perfusion without perfusion defects (e). LM, left main trunk; LAD, left anterior descending artery; DA1 and 2, the first and the second diagonal arteries; OMB, obtuse marginal branch; SA, short axis; HLA, horizontal long axis; VLA, vertical long axis.

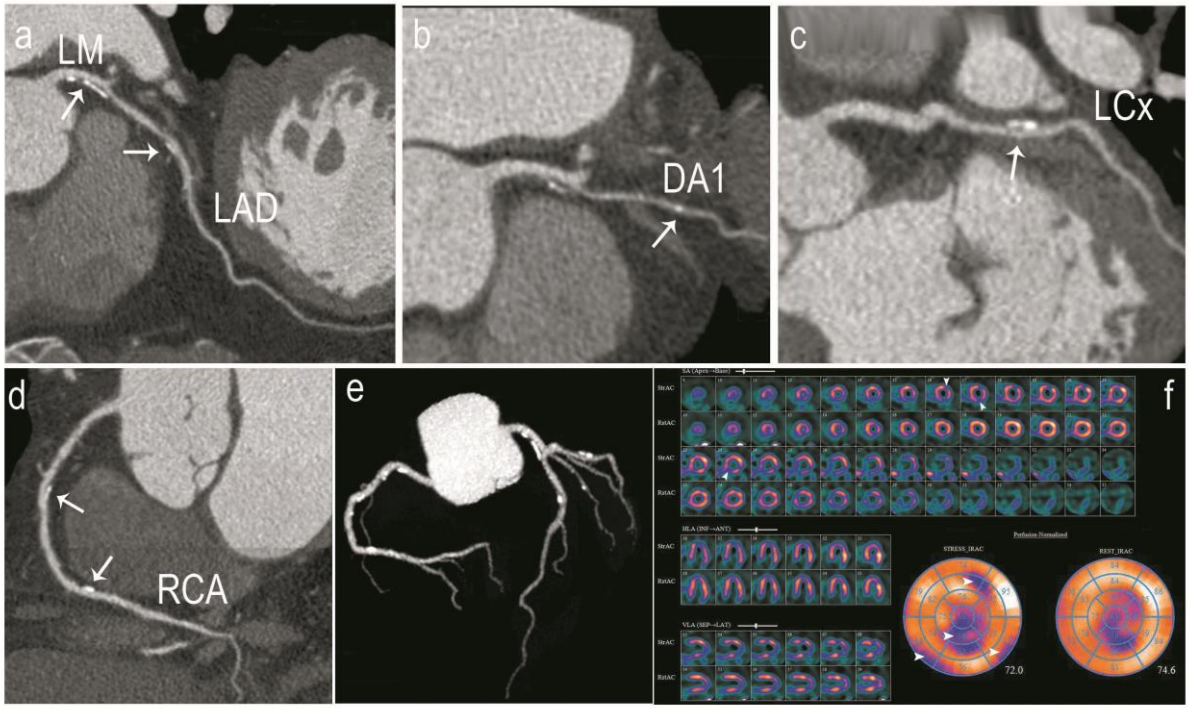

Figure 3. The example of discordance between CCTA and MPI results in 71-year-old man with nonanginal chest pain. Curved multiplanar reformations (a-d) and angiographic view (e) showing diffuse coronary artery disease without obstructive lesions in LM (a, e), DA1 (b, e), LCx (c, e), RCA (d, e). Segment involvement score – 7; Segment stenosis score – 11; CTA Risk Score 21.1. Cardiac perfusion stress/rest SPECT study and polar maps shows a predominately reversible perfusion defect within LAD, LCx and RCA territory (arrowheads). LM, left main trunk; LAD, left anterior descending artery; DA1, first diagonal artery; LCx, left circumflex artery; RCA, right coronary artery; SA, short axis; HLA, horizontal long axis; VLA, vertical long axis.

Neither the regional Segment Involvement Score, Segment Stenosis Score nor CTA Risk Score significantly correlated with the myocardial perfusion parameters in the LCx territory.

In the RCA territory, the regional Segment Involvement Score correlated weakly only with SSS (r=0.20, p=0.021). The Segment Stenosis Score had weak correlations with SSS (r=0.23, p=0.014). The CTA Risk Score also correlated only with SSS (r=0.29, p=0.023).

An example of an obstructive, but not ischemia-causing, coronary artery lesion in LAD is depicted in *Figure* 2. An example of diffuse atherosclerotic non-obstructive lesions is shown in *Figure* 3.

Discussion

The main findings of the study are: 1) the abnormalities of regional myocardial perfusion may develop frequently even in the absence of critical coronary artery lesions, presenting in a consistent proportion of patients with either absents of CT signs of coronary atherosclerosis and non-obstructive CAD. 2) there were revealed the only weak association between the extent of regional myocardial perfusion and integrated indexes of coronary atherosclerosis burden.

Coronary atherosclerosis and myocardial ischemia: a relationship beyond stenosis

It has been classically believed that regional myocardial inducible ischaemia might only develop in the presence of an angiographically obstructive coronary narrowing. As a matter of fact, classical data had demonstrated the existence of a relatively close relationship between the severity of a given coronary stenosis and downstream myocardial blood flow abnormalities, with a luminal narrowing >50-70% generally associating with the development of stress-induced ischaemia [3]. However, this statement has been repeatedly contradicted by more recent appraisals that have demonstrated conclusively that significant myocardial ischemia may frequently develop in the absence of anatomically significant coronary stenosis, and even in patients with normal coronary arteries, still associating with adverse prognosis [16-18]. Accordingly, while in patients with a non-obstructed coronary artery tree, the presence of myocardial perfusion abnormalities on MPI has been classically interpreted as a false positive finding of marginal, if any, clinical relevance, it has been solidly demonstrated that in many cases those alterations may rightfully indicate the presence of myocardial ischemia, as the result of endothelial/microvascular dysfunction and/or diffuse non significant CAD [19, 20]. The present study showed that more than in one-half of patients with unobstructed coronary arteries show the presence of stress-induced myocardial perfusion abnormalities on SPECT imaging, a proportion that increases to only 75% of the patients with significant CAD (≥50% luminal narrowing). All perfusion abnormalities were reversible and had mild severity (SSS values <8). More likely, these perfusion defects were related to coronary microvascular disease rather than to non-significant coronary artery lesion [21]. Dynamic SPECT approach measuring coronary flow reserve may elucidate the causes of perfusion abnormalities in patients without significant coronary artery lesion [22-24].

Conversely, roughly in one-quarter of the patients with angiographically significant CAD did not reveal any sign of myocardial ischaemia, underlining the relevance of coronary functional assessment in case of any degree of coronary stenosis. Forementioned findings further stressing the inconsistent relationship between stenosis severity and downstream ischemic burden [25]. The discrepancy between the anatomical and ischemic burden of CAD in terms of outcomes was shown in the COURAGE trail [26]. In this context our result are in agreement with the study Park H et al., where the association of CCTA atherosclerotic plaque characteristics such as aggregate plaque volume and low attenuation plaque were the predictors of ischemia only for ≥50 stenosis but not for <50% [27].

The effect of diffuse coronary atherosclerosis on regional myocardial perfusion

Although usually underestimated, the possible impact of diffuse non-significant coronary atherosclerosis on myocardial blood flow regulation can be relevant, possibly associating with the development of stress-induced myocardial ischemia even in the absence of an anatomically critical coronary lesion [28, 29, 19, 20]. In fact, it has been already demonstrated that diffuse coronary atherosclerosis can be responsible for a gradual base-to-apex reduction of myocardial perfusion, demonstrated both on non-invasive and invasive essays, as a result of increased epicardial flow resistance [30]. In this context, CCTA allows the accurate evaluation of epicardial coronary anatomy, giving the chance to outline the presence of mild coronary plaques that would not be underestimated, if not unapparent, on invasive coronary angiography. Using this technology, it has been demonstrated that the burden of epicardial coronary atherosclerosis correlates linearly with downstream myocardial blood flow impairment on PET imaging, adding relevant information on the characterization of coronary hemodynamics [19, 31].

More recent evidence have further strengthened this concept by suggesting that, even in the absence of a focal coronary luminal narrowing, non-significant CAD can induce regional perfusion abnormalities on SPECT imaging, associating with reversible LV diastolic dysfunction, as a sign of ischemia-induced functional impairment [20].

In this context, the results of the present study show that measures of CAD burden derived at CCTA correlate significantly with the extent of inducible ischemia only in patients with obstructive CAD.

Similar results were confirmed on vessel-based analysis, particularly in the case of the LAD. In this respect, the wide variability of coronary individual coronary anatomy might explain the apparently absent correlation between CTCA and MPI regional parameters in the LCX coronary artery territory. In fact, it has been already reported that the LCX and RCA may frequently share the same territory of distribution, posing difficulties in the correct assignment of myocardial perfusion defects on MPI to the pertinent coronary artery [32]. Conversely, the territory of distribution of the LAD shows a limited variability in the different patients. Moreover, in our study, only 11 patients had left coronary dominance, and two of them had ≥50% coronary artery stenosis in the LCX, reducing the power of the analysis.

Accordingly, present and previous results confirm that myocardial ischemia may develop frequently in patients with various degree of CAD, being predicted more by the extent of coronary atherosclerosis than by its anatomical severity. In this setting, the integrated evaluation of coronary anatomy and function by means of combined CCTA and MPI allows

characterizing the specific perfusion patterns in patients with CAD, defining the relative weight of focal and diffuse atherosclerosis, and helping to plan targeted therapeutic strategies.

Conclusion

Our study showed that myocardial ischemia can develop relatively frequently in patients with the absence of coronary atherosclerosis and with non-obstructive CAD. As a matter of fact, even in patients with minimal coronary atherosclerosis, the abnormalities in myocardial perfusion occurred in almost one in two cases. On the contrary, up to one-quarter of patients with significant coronary luminal narrowing has normal myocardial perfusion. Those differences might be partly explained by the presence of diffuse coronary atherosclerosis, as well as by such risk factors as hypertension and diabetes mellitus.

Limitations

The main limitation of this study is the relatively small size of the study population and particularly the small number of patients with the absence of coronary atherosclerosis on CCTA. There were no available methods such as invasive or CT fractional flow reserve for assessment of ischemia. We also did not use quantitatively myocardial perfusion evaluation, i.e. SPECT-derived myocardial blood flow and coronary flow reserve. In this study, the 3D fusion of anatomical (CCTA) and functional imaging (SPECT myocardial perfusion) was not performed, possibly reducing the correlations between integrated indexes of the coronary artery atherosclerotic lesions and myocardial perfusion parameters [32]. Another limitation is that the degrees of stenosis in the coronary arteries were detected based on data of CCTA. However, the results of CCTA were of good and excellent quality in 80% of patients, which determines the accuracy of the stenosis degree assessment. The impact of cardiovascular risk factors on myocardial perfusion regulation cannot be excluded, and in particular hypertension and obesity might have affected negatively perfusion variables [16]. However, the analysis of such an interaction is beyond the scope of our study.

Ethical approval

The local research ethics committee approved this retrospective analysis of previously collected data and the absence of written informed consent requirement. The study protocol conforms to the ethical guidelines of the 1975 Declaration of Helsinki.

Acknowledgments

This work was supported by Government task № AAAA-A15-115123110026-3.

Conflict of interest

The authors declare that they have no conflicts of interest

References

1. Underwood SR, Anagnostopoulos C, Cerqueira M, Ell PJ, Flint EJ, Harbinson M, et al. Myocardial perfusion scintigraphy: the evidence. *Eur J Nucl Med Mol Imaging* 2004; 31(2): 261-291. https://doi.org/10.1007/s00259-003-1344-5.
2. Tamarappoo BK, Gutstein A, Cheng VY, Nakazato R, Gransar H, Dey D, et al. Assessment of the relationship between stenosis severity and distribution of coronary artery stenoses on multislice computed tomographic angiography and myocardial ischemia detected by single photon emission computed tomography. *J Nucl Cardiol* 2010; 17(5): 791-802. https://doi.org/10.1007/s12350-010-9230-6.
3. Gould KL, Johnson NP, Bateman TM, Beanlands RS, Bengel FM, Bober R, et al. Anatomic versus physiologic assessment of coronary artery disease. Role of coronary flow reserve, fractional flow reserve, and positron emission tomography imaging in revascularization decision-making. *J Am Coll Cardiol* 2013; 62(18): 1639-1653. https://doi.org/10.1016/j.jacc.2013.07.076.
4. Diamond GA, Forrester JS. Analysis of probability as an aid in the clinical diagnosis of coronary-artery disease. *N Engl J Med* 1979; 300 (24): 1350-1358. https://doi.org/10.1056/NEJM197906143002402.
5. Henzlova MJ, Cerqueira MD, Mahmarian JJ, Yao SS. Quality Assurance Committee of the American Society of Nuclear Cardiology. Stress protocols and tracers. *J Nucl Cardiol* 2006; 13(6): e80-90. https://doi.org/10.1016/j.nuclcard.2006.08.011.
6. Pazhenkottil AP, Ghadri JR, Nkoulou RN, Wolfrum M, Buechel RR, Küest SM, et al. Improved outcome prediction by SPECT myocardial perfusion imaging after CT attenuation correction. *J Nucl Med* 2011; 52(2): 196-200. https://doi.org/10.2967/jnumed.110.080580.
7. Agatston AS, Janowitz WR, Hildner FJ, Zusmer NR, Viamonte M, Detrano R. Quantification of coronary artery calcium using ultrafast computed tomography. *J Am Coll Cardiol* 1990; 15(4): 827-832. https://doi.org/10.1016/0735-1097(90)90282-t.
8. Austen WG, Edwards JE, Frye RL, Gensini GG, Gott VL, Griffith LS, et al. A reporting system on patients evaluated for coronary artery disease. Report of the Ad Hoc Committee for Grading of Coronary Artery Disease, Council on Cardiovascular Surgery, American Heart Association. *Circulation* 1975; 51(4 Suppl): 5-40. https://doi.org/10.1161/01.cir.51.4.5.
9. Achenbach S, Ropers D, Hoffmann U, MacNeill B, Baum U, Pohle K, et al. Assessment of coronary remodeling in stenotic and nonstenoticcoronary atherosclerotic lesions by multidetector spiral computed tomography. *J Am Coll Cardiol* 2004; 43(5): 842-847. https://doi.org/10.1016/j.jacc.2003.09.053.
10. de Graaf MA, Broersen A, Ahmed W, Kitslaar PH, J. Dijkstra, Kroft LJ, et al. Feasibility of an automated quantitative computed tomography angiography-derived risk score for risk stratification of patients with suspected coronary artery disease. *Am J Cardiol* 2014; 113(12): 1947-1955. https://doi.org/10.1016/j.amjcard.2014.03.034.
11. Andreini D, Pontone G, Mushtaq S, Gransar H, Conte E, Bartorelli AL, et al. Long-term prognostic impact of CT-Leaman score in patients with non-obstructive CAD: Results from the COronary CT Angiography EvaluatioN For Clinical Outcomes InteRnational Multicenter (CONFIRM) study. *Int J Cardiol* 2017; 231: 18-25. https://doi.org/10.1016/j.ijcard.2016.12.137.
12. Tesche C, Caruso D, De Cecco CN, Shuler DC, Rames JD, Albrecht MH, et al. Coronary computed tomography angiography-derived plaque quantification in patients with acute coronary syndrome. *Am J Cardiol* 2017; 119(5): 712-718. https://doi.org/10.1016/j.amjcard.2016.11.030.
13. Rispler S, Keidar Z, Ghersin E, Roguin A, Soil A, Dragu R, et al. Integrated single-photon emission computed tomography and computed tomography coronary angiography for the assessment of hemodynamically significant coronary artery lesions. *J Am Coll Cardiol* 2007; 49(10): 1059-1067. https://doi.org/10.1016/j.jacc.2006.10.069.
14. Hachamovitch R, Kang X, Amanullah AM, Abidov A, Hayes SW, Friedman JD, et al. Prognostic implications of myocardial perfusion single-photon emission computed tomography in the elderly. *Circulation* 2009; 120(22): 2197-2206. https://doi.org/10.1161/CIRCULATIONAHA.108.817387.
15. Pereztol-Valdés O, Candell-Riera J, Santana-Boado C, Angel J, Aguadé-Bruix S, Castell-Conesa J, et al. Correspondence between left ventricular 17 myocardial segments and coronary arteries. *Eur Heart J* 2005; 26(24): 2637-2643. https://doi.org/10.1093/eurheartj/ehi496.

16. Crea F, Camici PG, Bairey Merz CN. Coronary microvascular dysfunction: an update. *Eur Heart J* 2014; 35(17): 1101-1111. https://doi.org/10.1093/eurheartj/eht513.
17. Johnson NP, Kirkeeide RL, Gould KL. Same Lesion, Different Artery, Different FFR!? *JACC Cardiovasc Imaging* 2019; 12(4): 718-721. https://doi.org/10.1016/j.jcmg.2017.11.029.
18. Lee JM, Layland J, Jung JH, Lee HJ, Echavarria-Pinto M, Watkins S, et al. Integrated physiologic assessment of ischemic heart disease in real-world practice using index of microcirculatory resistance and fractional flow reserve: insights from the International Index of Microcirculatory Resistance Registry. *Circ Cardiovasc Interv* 2015; 8(11): e002857. https://doi.org/10.1161/CIRCINTERVENTIONS.115.002857.
19. Liga R, Marini C, Coceani M, Filidei E, Schlueter M, Bianchi M, et al. Structural abnormalities of the coronary arterial wall in addition to luminal narrowing-affect myocardial blood flow reserve. *J Nucl Med* 2011; 52(11): 1704-1712. https://doi.org/10.2967/jnumed.111.091009.
20. Gimelli A, Liga R, Pasanisi EM, Casagranda M, Marzullo P. Myocardial ischemia in the absence of obstructive coronary lesion: The role of post-stress diastolic dysfunction in detecting early coronary atherosclerosis. *J Nucl Cardiol* 2017; 24(5): 1542-1550. https://doi.org/10.1007/s12350-016-0456-9.
21. Manabe O, Naya M, Tamaki N. Feasibility of PET for the management of coronary artery disease: Comparison between CFR and FFR. *J Cardiol* 2017; 70(2): 135-140. https://doi.org/10.1016/j.jjcc.2017.03.002.
22. Agostini D, Marie PY, Ben-Haim S, Rouzet F, Songy B, Giordano A, et al. Performance of cardiac cadmium-zinc-telluride gamma camera imaging in coronary artery disease: a review from the cardiovascular committee of the European Association of Nuclear Medicine (EANM). *Eur J Nucl Med Mol Imaging* 2016; 43(13): 2423-2432. https://doi.org/10.1007/s00259-016-3467-5.
23. Wells RG, Timmins R, Klein R, Lockwood J, Marvin B, deKemp RA, et al. Dynamic SPECT measurement of absolute myocardial blood flow in a porcine model. *J Nucl Med* 2014; 55(10): 1685-1691. https://doi.org/10.2967/jnumed.114.139782.
24. Ben-Haim S, Murthy VL, Breault C, Allie R, Sitek A, Roth N, et al. Quantification of Myocardial Perfusion Reserve Using Dynamic SPECT Imaging in Humans: A Feasibility Study. *J Nucl Med* 2013; 54(6): 873-879. https://doi.org/10.2967/jnumed.112.109652.
25. Sato A, Hiroe M, Tamura M, Ohigashi H, Nozato T, Hikita H, et al. Quantitative Measures of Coronary Stenosis Severity by 64-Slice CT Angiography and Relation to Physiologic Significance of Perfusion in Nonobese Patients: Comparison with Stress Myocardial Perfusion Imaging. *J Nucl Med* 2008; 49(4): 564-572. https://doi.org/10.2967/jnumed.107.042481.
26. Mancini GBJ, Hartigan PM, Shaw LJ, Berman DS, Hayes SW, Bates ER, et al. Predicting outcome in the COURAGE trial (Clinical Outcomes Utilizing Revascularization and Aggressive Drug Evaluation): coronary anatomy versus ischemia. *JACC Cardiovasc Interv* 2014; 7(2): https://doi.org/10.1016/j.jcin.2013.10.017.
27. Park HB, Heo R, Ó Hartaigh B, Cho I, Gransar H, Nakazato R, et al. Atherosclerotic plaque characteristics by CT angiography identify coronary lesions that cause ischemia: a direct comparison to fractional flow reserve. *JACC Cardiovasc Imaging* 2015; 8(1): 1-10. https://doi.org/10.1016/j.jcmg.2014.11.002.
28. Hernandez-Pampaloni M, Keng FY, Kudo T, Sayre JS, Schelbert HR. Abnormal longitudinal, base-to-apex myocardial perfusion gradient by quantitative blood flow measurements in patients with coronary risk factors. *Circulation* 2001; 104(5): 527-532. https://doi.org/10.1161/hc3001.093503.
29. Johnson NP, Gould KL. Clinical evaluation of a new concept: resting myocardial perfusion heterogeneity quantified by markovian analysis of PET identifies coronary microvascular dysfunction and early atherosclerosis in 1,034 subjects. *J Nucl Med* 2005; 46(9): 1427-1437. https://www.ncbi.nlm.nih.gov/pubmed/16157524.
30. De Bruyne B, Hersbach F, Pijls NH, Bartunek J, Bech JW, Heyndrickx GR, et al. Abnormal epicardial coronary resistance in patients with diffuse atherosclerosis but "Normal" coronary angiography. *Circulation* 2001; 104(20): 2401-2406. https://doi.org/10.1161/hc4501.099316.
31. Naya M, Murthy VL, Blankstein R, Sitek A, Hainer J, Foster C, et al. Quantitative Relationship Between the Extent and Morphology of Coronary Atherosclerotic Plaque and Downstream Myocardial Perfusion. *J Am Coll Cardiol* 2011; 58(17): 1807-1816. https://doi.org/10.1016/j.jacc.2011.06.051.
32. Liga R, Vontobel J, Rovai D, Marinelli M, Caselli C, Pietila M, et al. Multicentre multi-device hybrid imaging study of coronary artery disease: results from the EValuation of INtegrated Cardiac Imaging for the Detection and Characterization of Ischaemic Heart Disease (EVINCI) hybrid imaging population. *Eur Heart J Cardiovasc Imaging* 2016; 17(9): 951-960. https://doi.org/10.1093/ehjci/jew038.

Authors:
Konstantin V. Zavadovsky – MD, Head of Department of Nuclear Medicine, Cardiology Research Institute, Tomsk National Research Medical Centre, Tomsk, Russia. https://orcid.org/0000-0002-1513-8614.
Alina N. Maltseva – Radiology Resident, Department of Nuclear Medicine, Cardiology Research Institute, Tomsk National Research Medical Centre, Tomsk, Russia. https://orcid.org/0000-0002-1311-0378.
Elena V. Grakova – MD, Leading Researcher, Department of Myocardial Pathology, Cardiology Research Institute, Tomsk National Research Medical Centre, Tomsk, Russia. https://orcid.org/0000-0003-4019-3735.
Kristina V. Kopeva – PhD, Junior Researcher, Department of Myocardial Pathology, Cardiology Research Institute, Tomsk National Research Medical Centre, Russian Academy of Sciences, Tomsk, Russia. https://orcid.org/0000-0002-2285-6438.
Marina O. Gulya – PhD, Radiologist, Department of Nuclear Medicine, Cardiology Research Institute, Tomsk National Research Medical Centre, Tomsk, Russia. https://orcid.org/0000-0001-5689-9754.
Victor V. Saushkin – PhD, Senior Researcher, Department of Nuclear Medicine, Cardiology Research Institute, Tomsk National Research Medical Centre, Tomsk, Russia. https://orcid.org/0000-0001-5564-3802.
Andrew V. Mochula – PhD, Researcher, Department of Nuclear Medicine, Cardiology Research Institute, Tomsk National Research Medical Centre, Tomsk, Russia. https://orcid.org/0000-0003-0883-466X.
Riccardo Liga – MD, Cardiologist, Cardio-Thoracic and Vascular Department, University Hospital of Pisa, Pisa, Italy. https://orcid.org/0000-0002-9964-5604.
Alessia Gimelli – MD, Head of Nuclear Cardiology Unit, Fondazione Toscana G. Monasterio, Pisa, Italy. https://orcid.org/0000-0003-3378-1723.